JOURNAL OF BACTERIOLOGY, Dec. 2006, p. 8054–8061 Vol. 188, No. 23
0021-9193/06/$08.00+0 doi:10.1128/JB.00935-06

Characterization of *myo*-Inositol Utilization by *Corynebacterium glutamicum*: the Stimulon, Identification of Transporters, and Influence on L-Lysine Formation[▽]

Eva Krings,[1] Karin Krumbach,[1] Brigitte Bathe,[2] Ralf Kelle,[2] Volker F. Wendisch,[3] Hermann Sahm,[1] and Lothar Eggeling[1]*

Institute of Biotechnology, Research Centre Juelich, D-52425 Juelich, Germany[1]; Degussa R&D Feed Additives/Biotechnology, P.O. Box 1112, D-33788 Halle, Germany[2]; and Institute of Molecular Microbiology and Biotechnology, University of Münster, Corrensstrasse 3, D-48149 Münster, Germany[3]

Received 28 June 2006/Accepted 18 September 2006

Although numerous bacteria possess genes annotated *iol* in their genomes, there have been very few studies on the possibly associated *myo*-inositol metabolism and its significance for the cell. We found that *Corynebacterium glutamicum* utilizes *myo*-inositol as a carbon and energy source, enabling proliferation with a high maximum rate of 0.35 h^{-1}. Whole-genome DNA microarray analysis revealed that 31 genes respond to *myo*-inositol utilization, with 21 of them being localized in two clusters of >14 kb. A set of genomic mutations and functional studies yielded the result that some genes in the two clusters are redundant, and only cluster I is necessary for catabolizing the polyol. There are three genes which encode carriers belonging to the major facilitator superfamily and which exhibit a >12-fold increased mRNA level on *myo*-inositol. As revealed by mutant characterizations, one carrier is not involved in *myo*-inositol uptake whereas the other two are active and can completely replace each other with apparent K_ms for *myo*-inositol as a substrate of 0.20 mM and 0.45 mM, respectively. Interestingly, upon utilization of *myo*-inositol, the L-lysine yield is 0.10 mol/mol, as opposed to 0.30 mol/mol, with glucose as the substrate. This is probably not only due to *myo*-inositol metabolism alone since a mixture of 187 mM glucose and 17 mM *myo*-inositol, where the polyol only contributes 8% of the total carbon, reduced the L-lysine yield by 29%. Moreover, genome comparisons with other bacteria highlight the core genes required for growth on *myo*-inositol, whose metabolism is still weakly defined.

Inositol is a building block of plants and is thus probably one of the sources of traces of *myo*-inositol, or its phosphorylated derivative *myo*-inositol hexakisphosphate, in soil (26). Accordingly, there are indications that a number of microorganisms are able to utilize *myo*-inositol. For instance, the soil-inhabiting *Rhizobiaceae* family members *Sinorhizobium fredii* (16) and *Rhizobium leguminosarum* (9) have the ability to catabolize or even grow on *myo*-inositol and this feature may increase their fitness for better nodulating the host plant (10). Also, *Klebsiella* (*Aerobacter*) *aerogenes* is able to utilize *myo*-inositol (19) and early biochemical work with this organism established how the polyol could be metabolized (2) (Fig. 1).

As can be seen from their genome sequences, a large number of bacteria have genes which are annotated as *iol* genes. These are often clustered, for example, the *iolDEB* genes in *R. leguminosarum*, which are required for growth on inositol (9), or in *Clostridium perfringens*, where a cluster of 13 genes is induced by *myo*-inositol with the participation of the regulator IolR (17). In *Bacillus subtilis*, there is an *iol* divergon comprising *iolABCDEFGHIJ* and *iolRS* whose repression by glucose is in part CcpA dependent (29, 30). Relatively few studies have been done to demonstrate the participation of the *iol* genes in inositol metabolism, and there are a very limited number of biochemical studies on their enzyme function. A *myo*-inositol dehydrogenase has been identified that initiates *myo*-inositol metabolism. The enzyme is encoded by *iolG* of *B. subtilis* (10) or *idhA* in *Sinorhizobium meliloti* (11), respectively, as well as *S. fredii* (16). In *S. meliloti*, its inactivation was found to disable *myo*-inositol utilization (11). The second gene function identified is that of *iolE*, which encodes a 2-keto-*myo*-inositol dehydratase (31). Import of the polyol is known to be catalyzed by transporters belonging to the major facilitator superfamily. In *B. subtilis*, two such *myo*-inositol uptake carriers are present (28), with *iolF* located within the *iolABCDEFGHIJ* operon representing the minor transporter for uptake. The second transporter, *iolT*, is located elsewhere in the chromosome, and its inactivation causes reduced growth on a number of carbon sources, with the most pronounced effect on *myo*-inositol (28).

We are interested in *Corynebacterium glutamicum*, an apathogenic bacterium of industrial interest used for the large-scale production of amino acids, in particular, L-glutamate and L-lysine (8). Together with *Mycobacterium tuberculosis*, for instance, this bacterium belongs to the suborder *Corynebacterineae*, characterized among others by possessing *myo*-inositol as a cellular building block, as is the case in eukaryotes (20, 22). The inositol is required for the synthesis of phosphatidyl-*myo*-inositol, which is an abundant phospholipid in the cytoplasmic membrane and which in turn is also a precursor of more-complex cellular glycolipids in *Corynebacterineae* such as lipomannans and lipoarabinomannans (5). Furthermore, *myo*-inositol is also a building block for mycothiol (5, 7, 22), which is a low-molecular-mass thiol specific to *Corynebacterineae* and necessary for protection against the damaging effects of reac-

* Corresponding author. Mailing address: Institute of Biotechnology, Research Centre Juelich, D-52425 Juelich, Germany. Phone: 0049 2461 615132. Fax: 00492461612710. E-mail: l.eggeling@fz-juelich.de.
▽ Published ahead of print on 22 September 2006.

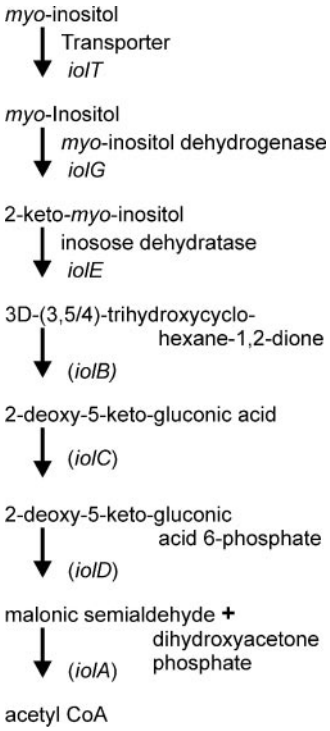

FIG. 1. Assumed pathway for *myo*-inositol degradation. The pathway is in part speculative and largely based on enzymological studies of *K. aerogenes* (2, 19), studies of *B. subtilis* (27–30), and genome comparisons. The genes and the enzymes encoded are given; those with a presumed assignment are in parentheses.

tive oxygen species, similar to glutathione in eukaryotes and gram-negative bacteria. In *C. glutamicum*, we detected a number of genes annotated as *iol* and wished to know whether their presence enables *C. glutamicum* to grow on this polyol with an additional focus on the transport of *myo*-inositol and the physiological consequences of its utilization.

MATERIALS AND METHODS

Bacteria, plasmids, oligonucleotides, and culture conditions. All of the strains, plasmids, and oligonucleotides used in this study are described in Table 1. The minimal medium used for *C. glutamicum* was CGXII (8), which contained the carbon source glucose or *myo*-inositol autoclaved separately. *C. glutamicum* was grown as 50-ml cultures in 500-ml baffled Erlenmeyer flasks on a rotary shaker at 120 rpm. Growth of the bacteria was monitored by measuring the optical density at 600 nm (OD_{600}).

Recombinant DNA work. Standard protocols were applied for the generation of fragments via PCR, ligation, and restriction (21), with each plasmid made verified by sequencing. The chromosomal mutations of *C. glutamicum* were made by introducing the nonreplicative plasmids via electroporation. For in-frame deletions, the clones with an integrated vector were subsequently selected for absence of the vector due to the lethal *sacB* function of pK19*mobsacB* (23).

Preparation of total RNA and DNA microarray analyses. Cultures were grown in CGXII minimal medium containing 40 g liter^{-1} *myo*-inositol or glucose. In the exponential growth phase at an OD_{600} of 4 to 6, 25 ml of each culture was used for the preparation of total RNA as previously described (27). Isolated RNA samples were analyzed for quantity and quality by UV spectrophotometry and denaturing formaldehyde agarose gel electrophoresis (21), respectively, and stored at −70°C until use. The generation of whole-genome DNA microarrays, synthesis of fluorescently labeled cDNA from total RNA, microarray hybridization, washing, and data analysis were performed as described previously (27). Genes that exhibited significantly changed mRNA levels ($P < 0.05$ by Student's *t* test) by at least a factor of 2.8 were determined in independent growth experiments with subsequent hybridizations (Table 2).

Uptake measurements. For determination of *myo*-inositol uptake, cultures grown overnight on CGXII with *myo*-inositol were diluted in fresh medium and grown to an OD_{600} of approximately 4 to 6. Cells were washed twice with cold CGXII medium without *myo*-inositol, the OD_{600} was adjusted to 5 (corresponding to 1.2 mg [dry weight] ml^{-1}), and the cells were stored on ice. A 0.9-ml volume of this cell suspension was equilibrated for 4 min at 25°C by stirring in a water bath. Uptake was initiated by the addition of 100 μl of an inositol mixture containing 5 to 500 nmol *myo*-inositol and 5 μl *myo*-[1,2-^{3}H(N)]-inositol (1 mCi/ml; Biotrend Chemicals, Cologne, Germany). Aliquots of 100 μl were taken after 10, 25, 40, and 55 s, and individually processed by drawing through a prewetted glass fiber filter (Millipore catalog no. APFF02500) placed on a vacuum manifold. Cells were immediately washed with 2 × 2.5 ml ice-cold 1 M LiCl. Radioactivity was quantified by liquid scintillation counting on a Tri-Carb 1600CA in Instant Scin-Gel Plus (Packard catalog no. 6013398). The uptake was usually linear over time, but for concentrations below 0.25 mM *myo*-inositol, only uptake up to 40 s was considered. The kinetic data were analyzed via nonlinear regression according to the Michaelis-Menten equation.

RESULTS

Growth on *myo*-inositol. In microarray studies with *C. glutamicum* with the transcriptional regulator *lysG* deleted (4), we occasionally noted altered mRNA levels of genes putatively related to *myo*-inositol utilization. We therefore assayed *C. glutamicum* for the ability to utilize this polyol. When *C. glutamicum* was inoculated into the salt medium CGXII containing 40 g liter^{-1} *myo*-inositol as the sole carbon and energy source, after a short lag, a high growth rate of 0.35 h^{-1} was obtained (Fig. 2A). This was close to that on glucose (0.41 h^{-1}). The short lag phase observed on *myo*-inositol is due to the use of glucose-grown cells for inoculation, since it was absent in cells pregrown in inositol (data not shown). On a mixture of both sugars, each at 2 g liter^{-1}, the growth rate was 0.41 h^{-1} with no observable diauxie. This indicates an efficient molecular and enzymological machinery of *C. glutamicum* for using *myo*-inositol as efficiently as more common carbon sources in laboratory use like glucose, ribose, acetate, or lactate, for instance.

Transcriptome analysis. In order to determine the effect of *myo*-inositol utilization on global gene expression, whole-genome DNA microarrays of *C. glutamicum* were used (27). The determination of the mRNA population of cells grown with *myo*-inositol compared to cells grown with glucose resulted in a relatively small number of 31 genes exhibiting an at least 2.8-fold change in their transcript level. Among those reduced are *mez*, encoding malic enzyme, and *sucC*, encoding the β-chain of succinyl-coenzyme A (CoA) synthetase (Table 2). When the threshold was set to 2 (data not shown), also *ptsS*, encoding the sucrose-specific IIABC component of the phosphotransferase system, and *ptsM*, which encodes the glucose-specific IIABC component, exhibited a significantly reduced level, a fact indicating significant carbon source-dependent regulation of the genes of the central metabolism.

The most strongly reduced mRNA level during growth on *myo*-inositol was determined for the *myo*-inositol-1-phosphate synthase gene, *ips* (20). This gene is required in *Corynebacterineae* for glucose 6-phosphate conversion to *myo*-inositol, which is a constituent of mycothiol and phosphatidyl-*myo*-inositol. A regulation of *ips* is not yet known, but its repression is consistent with the fact that an external supply of *myo*-inositol makes its cellular synthesis dispensable.

TABLE 1. Strains, plasmids, and oligonucleotides used in this study

Strain, plasmid, or oligonucleotide[a]	Relevant characteristic(s) or sequence[b]	Source, reference, or purpose
C. glutamicum strains		
ATCC 13032	WT	Culture collection
ATCC 21527	Lysine producer obtained by undirected mutagenesis	Culture collection
MH20-22B	Lysine producer obtained by undirected mutagenesis	24
DM1730	Lysine producer; *pyc*P458S *hom*V59A *lysC*T311I *zwf*A243T	13
WTΔ*iolD*	In-frame deletion of *iolD*	This work
WT::p*iolG′*	Vector integrated into *iolG*	This work
WTΔ*oxiII*	In-frame deletion of *oxiC-oxiE*	This work
WTΔ*iolII*	In-frame deletion of *adhA-oxiE*	This work
WTΔ*oxiII*::p*iolG′*	In-frame deletion of *oxiC-oxiE* and vector integrated into *iolG*	This work
WTΔ*iolT1*	In-frame deletion of *iolT1*	This work
WTΔ*iolT2*	In-frame deletion of *iolT2*	This work
WTΔ*iolT1*Δ*iolT2*	In-frame deletion of *iolT1* and *iolT2*	This work
Plasmids		
pK19mobsacB	Km^r; mobilizable (*oriT*); *oriV*	23
pT18mob2	Tet^r; mobilizable (*oriT*); *oriV*	23
pK19mobsacBΔ*iolD*	Vector enabling deletion of 1,861 bp of *iolD*	This work
pT18mob2::p*iolG′*	Vector used to integrate 408 bp into *iolG*	This work
pK19mobsacBΔ*oxi*II	Vector enabling deletion of 4,072 bp of cluster II	This work
pK19mobsacBΔ*iol*II	Vector enabling deletion of 8,799 bp of cluster II	This work
pK19mobsacBΔ*iol*T1	Vector enabling deletion of 1,422 bp of *iolT1*	This work
pK19mobsacBΔ*iol*T2	Vector enabling deletion of 1,472 bp of *iolT2*	This work
p*iolG′*	Vector pK19mobsacB with internal fragment of *iolG* enabling its disruption	This work
Oligonucleotides		
iolD_No	5′-CGCGGATCCAAGTAATCACCCCAGGTGAAAACTGGAG-3′	Primer for 1,861-bp *iolD* deletion (BamHI)
iolD_Co	5′-CGCGGATCCAACGAGGTGCTCAGCACCCAGC-3′	Primer for1,861-bp *iolD* deletion (BamHI)
iolD_Ni	5′-CCCATCCACTAAACTTAAACATCTCTTCGTTTCAGCCATG AAATTTTA-3′	Primer for 1,861-bp *iolD* deletion
iolD_Ci	5′-TGTTTAAGTTTAGTGGATGGGAAAAACCAAGCCCTCCAG CGTCC-3′	Primer for 1,861-bp *iolD* deletion
iolG_U1B	5′-CGC GGA TCC GCG CGG CGA AGC TGG CGA ACT GC-3′	Primer for *iolG* disruption (BamHI)
iolG_L1B	5′-CGCGGATCCGCGCGGTAGCGAAACGGGTGGTGA-3′	Primer for *iolG* disruption (BamHI)
oxiII_No	5′-TCCCCCCGGGGGATCGCCGCTGTAGGAGCAC-3′	Primer for 4,072-bp deletion (SmaI)
oxiII_Co	5′-TCCCCCCGGGGGTTAGGCAGGATGAGGTTGAGAa-3′	Primer for 4,072-bp deletion (SmaI)
oxiII_Ni	5′-CCCATCCACTAAACTTAAACAAATTTTTTGATCACTCATG GGAATTCT-3′	Primer for 4,072-bp deletion
oxiII_Ci	5′-TGTTTAAGTTTAGTGGATGGGCCAGTTGAGGTGCGTGCG CTG-3′	Primer for 4,072-bp deletion
iol II_No	5′-CGCGGATCCGATACGAGCATTCGGAACGGGA-3′	Primer for 8,799-bp deletion (BamHI)
iolII_Co	5′-GCGGGATCCCAGTCCGAGCTTTGAGATGTTC-3′	Primer for 8,799-bp deletion (BamHI)
iolII_Ni	5′-CCCATCCACTAAACTTAAACAGATCCGGCAGTTCTTAGC GCA-3′	Primer for 8,799-bp deletion
iolII_Ci	5′-TGTTTAAGTTTAGTGGATGGGCCAGTTGAGGTGCGTGCG CT-3′	Primer for 8,799-bp deletion
iolT1_No	5′-CGCGGATCCCTGAGTCGTCGTATTATTGCGTATTTT-3′	Primer for 1,422-bp deletion (BamHI)
iolT1_Co	5′-CGCGGATCCACATTAGGATCTTTAAGCAGTGAATGA-3′	Primer for 1,422-bp deletion (BamHI)
iolT1_Ni	5′-CCCATCCACTAAACTTAAACAAAAGGAAAGGTGCACTAA AAACCCAG-3′	Primer for 1,422-bp deletion
iolT1_Ci	5′-TGTTTAAGTTTAGTGGATGGGTTTCAGGGCTGTCGGCCT GAATGA-3′	Primer for 1,422-bp deletion
iolT2_No	5′-CCGGAATTCTGCTTTGGCCAAACCTATGGTGGA-3′	Primer for 1,472-bp deletion (BamHI)
iollT2_Co	5′-CCGGAATTCACGGCTAAACAGGTTGTCTTGGGTA-3′	Primer for 1,472-bp deletion (BamHI)
iolTII_Ni	5′-CCCATCCACTAAACTTAAACAATCTTCAAGAAGGCTTAA ACCCCCT-3′	Primer for 1,472-bp deletion
iolTII_Ci	5′-TGTTTAAGTTTAGTGGATGGGGGCCGATGTACTTGATGT GGCCTT-3′	Primer for 1,472-bp deletion

[a] No, N-terminal outer primer; Co, C-terminal outer primer; Ni, N-terminal inner primer; Ci, C-terminal inner primer.
[b] Restriction sites in the oligonucleotides are underlined.

Twenty-one genes showed an up to 18-fold increase in mRNA level, indicative of a possible function within *myo*-inositol catabolism (Table 2). All but one of these genes are located in two large clusters. The exception is NCgl2865, predicted to encode a secreted protein containing three copper oxidase-like domains. The genome organization of the two clusters is given in Fig. 3, where genes which showed a ≥2.8-fold increase in mRNA level are marked in black. The core of

TABLE 2. Genes of *C. glutamicum* whose average mRNA ratio was altered ≥2.8-fold ($P \leq 0.05$) in *myo*-inositol-grown cells compared to that in glucose-grown cells in at least three independent cultivations

NCBI[a] designation	Open reading frame	Annotation	Gene	mRNA ratio[b]	
				Inositol vs Glucose	BHI vs CGXII
NCgl0029	Cgl0030	ABC transporter/periplasmic D-ribose-binding protein	*rbsB*	0.19	0.38
NCgl0155	Cgl0158	*myo*-Inositol catabolism, carbohydrate kinase	*iolC*	4.94	3.07
NCgl0157	Cgl0160	*myo*-Inositol catabolism, aldehyde dehydrogenase	*iolA*	16.65	7.16
NCgl0158	Cgl0161	*myo*-Inositol catabolism	*iolB*	16.55	15.04
NCgl0159	Cgl0162	*myo*-Inositol catabolism, thiamine pyrophosphate-requiring enzyme	*iolD*	12.01	4.66
NCgl0160	Cgl0163	2-Keto-*myo*-inositol dehydratase	*iolE*	18.64	13.93
NCgl0161	Cgl0164	*myo*-Inositol dehydrogenase, oxidoreductase	*iolG*	16.55	7.38
NCgl0162	Cgl0165	*myo*-Inositol catabolism, isomerases/epimerase	*iolH*	8.32	3.69
NCgl0163	Cgl0166	Efflux carrier, major facilitator superfamily; MFS1		17.33	2.33
NCgl0164	Cgl0167	*myo*-Inositol dehydrogenase, oxidoreductase	*oxi1*	2.85	0.88
NCgl0167	Cgl0170	Transcriptional regulator, LacI type; LacI1		7.93	4.07
NCgl0168	Cgl0171	Putative oxidoreductase dehydrogenases	*oxiB*	9.37	5.14
NCgl0178	Cgl0181	*myo*-Inositol transporter	*iolT1*	12.86	7.17
NCgl0697	Cgl0727	Trehalose/maltose-binding protein; *malE*		0.25	2.53
NCgl0916	Cgl0954	γ-Glutamyltransferase; *ggt*		0.34	1.34
NCgl0933	Cgl0972	Porin	*porB*	0.25	2.52
NCgl1368	Cgl1423	Putative acetyltransferase		0.21	3.36
NCgl1917	Cgl1992	ABC transporter/oligopeptide permease; *oppC*		0.29	2.63
NCgl2477	Cgl2566	Succinyl-CoA synthetase (beta chain)	*sucC*	0.23	1.53
NCgl2865	Cgl2967	Secreted multicopper oxidase; *cumA*		4.40	1.29
NCgl2894	Cgl2996	*myo*-Inositol-1-phosphate synthase	*ips*	0.09	0.17
NCgl2904	Cgl3007	Malic enzyme	*mez*	0.33	3.27
NCgl2951	Cgl3056	Hydroxyquinol 1,2-dioxygenase; *catA*		9.48	2.12
NCgl2952	Cgl3057	Iron-containing alcohol dehydrogenase, oxidoreductase; *adh1*		7.56	7.27
NCgl2953	Cgl3058	*myo*-Inositol transporter	*iolT2*	13.94	6.19
NCgl2955	Cgl3060	*myo*-Inositol dehydrogenase	*oxiC*	18.83	9.85
NCgl2956	Cgl3061	*myo*-Inositol catabolism, sugar phosphate isomerase/epimerase		21.02	8.67
NCgl2957	Cgl3062	*myo*-Inositol dehydrogenase	*oxiD*	26.83	9.53
NCgl2958	Cgl3063	*myo*-Inositol dehydrogenase	*oxiE*	12.54	3.04
NCgl2959	Cgl3064	Secreted phosphoesterase		4.34	0.6
NCgl2961	Cgl3066	Proline/ectoine carrier	*proP*	0.30	0.83

[a] Numbers for the corresponding open reading frames of the *C. glutamicum* genome NC_003450 are given. NCBI, National Center for Biotechnology Information.
[b] The first column gives the mRNA ratio for genes of *C. glutamicum* ATCC 13032 grown on *myo*-inositol to that of cells grown on glucose. The far right column gives the ratios for BHI- versus CGXII-glucose grown cells, and data are limited to those genes where *myo*-inositol utilization already revealed altered mRNA levels.

cluster I spans about 16 kb and comprises 13 genes (Fig. 3). It partly resembles the *iol* cluster of *B. subtilis* (29), and the *iol* gene annotations were used according to that introduced for this organism, although definite functions are unknown in almost all cases. The mRNA level of NCgl0156, located between *iolC* and *iolA*, was also slightly increased but less than 2.8-fold. An orthologue of this gene is not present in *B. subtilis*. It is most likely that the 10 genes of *C. glutamicum* from *iolC* to *oxiA* are cotranscribed as an operon. In contrast, the LacI-type regulator encoded by NCgl0167 (Reg1 in Fig. 3) and divergently transcribed *oxiB*, as well as remotely located *iolT1*, all three with an mRNA level of ≥7, might be separately transcribed.

Cluster II spans about 14.6 kb and consists of eight genes which also exhibited a ≥2.8-fold increase in mRNA level. Only the level of the putative regulator gene *iclR*, located in front of the cluster of genes encoding three oxidoreductases, was not increased during growth on *myo*-inositol.

We also wanted to know whether mRNA levels of cells grown on complex medium consisting of brain heart extract (BHI) also influence *iol* gene expression and compared the mRNA levels of cells grown on BHI with those of cells grown on CGXII salt medium containing glucose (Table 2). Indeed, a number of *iol* genes responded and *ips* was downregulated, suggesting that inositol utilization is part of cell mass generation during growth on the complex medium BHI. This is in agreement with the detection of two Iol proteins of *C. glutamicum* grown on complex medium (15).

Characterization of selected *iol* mutants. The large number of genes apparently related to *myo*-inositol catabolism in *C. glutamicum* is intriguing. Unfortunately, functional studies of enzymes and genes of inositol metabolism are scarce (Fig. 1). However, cleavage of the putative intermediate 2-deoxy-5-keto-D-gluconic acid is considered a key step in *myo*-inositol metabolism, as shown in the early studies of *K. aerogenes* by Anderson and Magasanik (2). Since cleavage of α-ketols in carbohydrate metabolism is typically performed by thiamine-pyrophosphate-dependent enzymes and the *iolD* gene product of *C. glutamicum* possesses a corresponding binding site (not shown), a vector was constructed to delete this gene from the wild type (WT) of *C. glutamicum* (see Materials and Methods). The resulting mutant, WTΔ*iolD*, was unable to grow on *myo*-inositol, whereas growth on glucose was hardly affected (Fig. 2B). Thus, *iolD* within cluster I is essential for *myo*-inositol utilization by *C. glutamicum*.

As many as six genes for oxidoreductases have increased expression levels upon *myo*-inositol utilization. PFAM analysis (3) identified three oxidoreductases (*iolG*, *oxiA*, *oxiB*) within

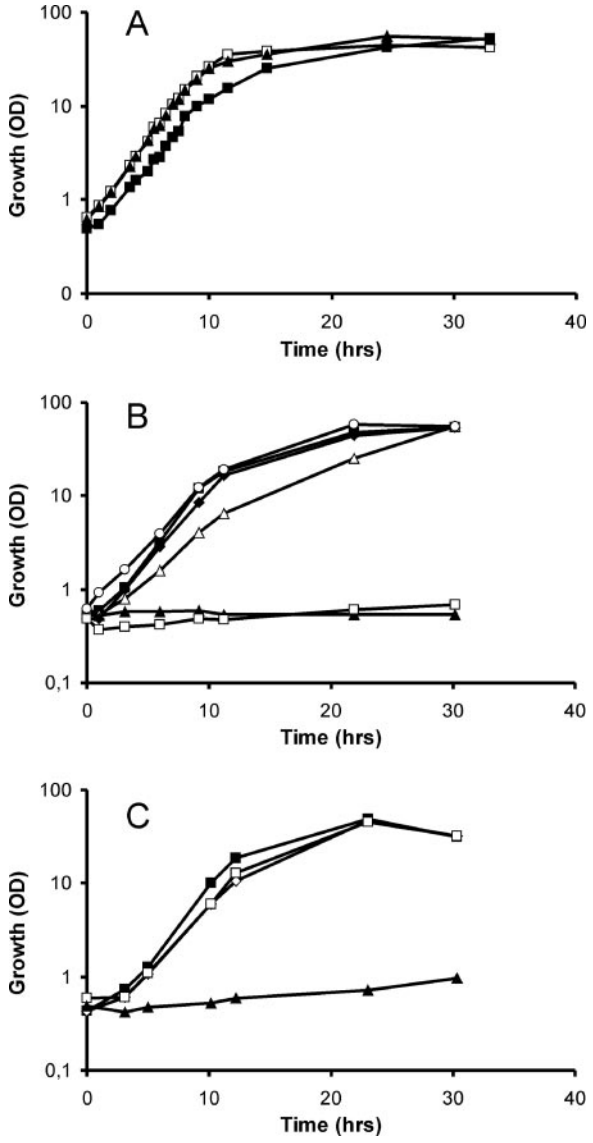

FIG. 2. Growth of *C. glutamicum* WT and mutants generated in this study on *myo*-inositol and glucose. (A) Growth of the WT on 4% glucose (□), on 4% *myo*-inositol (■), and on a mixture (2% plus 2%) of the two sugars (▲). (B) Growth of the Δ*iolD* mutant on *myo*-inositol (□) and glucose (○). Growth of the Δ*oxiII* mutant (◆), the p*iolG′* mutant (△), and the Δ*oxiII*::p*iolG′* double mutant (▲) on *myo*-inositol is compared to that of the WT on *myo*-inositol (■). (C) Growth of the transporter deletion mutants Δ*iolT1* (□), Δ*iolT2* (◇), and Δ*iolT1*Δ*iolT2* (▲) compared to that of the WT on *myo*-inositol (■).

cluster I and an additional three in cluster II (*oxiC*, *oxiD*, *oxiE*). Since a *iolG* orthologue is present within the *B. subtilis iol* operon (39% identities), we inactivated the orthologue to generate strain WT::p*iolG′*. As shown in Fig. 2B, its growth on inositol was reduced compared to that of the control but was still possible. Therefore, we considered that one of the other oxidoreductases might partially substitute for the function of *iolG*. IolG exhibits identities of 27% to OxiE, 22% to OxiD, and still 19% to OxiC over the entire lengths of the proteins, whereas identities to OxiA and OxiB were significantly less. The oxidoreductase encoded by *idhA* of *S. meliloti* (11) is, apart from *iolE* of *B. subtilis* (31), the only functionally identified gene of bacterial inositol metabolism, and OxiE, OxiD, and OxiC in cluster II exhibit high identities to IdhA but low identities to OxiA and OxiB. We therefore considered that the three oxidoreductases in cluster II might have some overlapping activity with the function of *iolG* and constructed plasmid pK19mobsacBΔ*oxiII* to delete the 4.072-kb region of cluster II encompassing *oxiC* to *oxiE* (Fig. 3). The growth of generated strain WTΔ*oxiII* is shown in Fig. 2B. Growth on neither inositol nor glucose (not shown) was influenced by the deletion. We subsequently inactivated *iolG* in the strain with the four genes of cluster II deleted to generate WTΔ*oxiII*::p*iolG′*. This strain was no longer able to grow on *myo*-inositol. This result indicates that the genes of cluster II play a subordinate role in *myo*-inositol utilization and that apparently a number of overlapping oxidoreductase activities exist in *C. glutamicum* which can be used to enable growth on this carbon source. Due to the growth characteristics of WTΔ*oxiII*::p*iolG′*, we hypothesized that further genes of cluster II might be redundant or unnecessary for *myo*-inositol utilization. To this end, plasmid pK19mobsacBΔ*iolII* was constructed and the 8.799-kb chromosomal region extending from *adhA* to *oxiE* (Fig. 3) was deleted to generate WTΔ*iolII*. Growth on *myo*-inositol was not reduced by this deletion either (not shown), which indicates that cluster II is dispensable for *myo*-inositol metabolism and that the corresponding genes might play an as-yet-undiscovered role or indicate ongoing evolution although the data show that they are at least in part functional.

Characterization of transporter mutants. There are three carrier genes which exhibit an at least 12-fold increase in the mRNA level upon *myo*-inositol utilization: *mfs* in cluster I, remote gene *iolT1*, and *iolT2* in cluster II (Fig. 3). All transporters belong to the major facilitator superfamily and exhibit identities to sugar transporters or, in the case of *mfs*, also identities to annotated efflux carriers. The presence of three transporters resembles the situation in *B. subtilis*, which possesses two transporters for inositol uptake (28). To move toward an analysis of the function of the transporters in *C. glutamicum*, we inactivated each of these three genes individually in strain ATCC 21527, an L-lysine producer, but growth was not hampered on CGXII plates containing as a carbon source sorbitol, glucose, ribose, fructose, arabitol, gluconate, or saccharose (each at 40 g liter^{-1}) compared to that of controls (not shown). Following this observation, we deleted the transporter genes *iolT1* and *iolT2* in *C. glutamicum* strain ATCC 13032 (WT) individually and together. The growth of the resulting strains is shown in Fig. 2C. Whereas the growth of WTΔ*iolT1* and WTΔ*iolT2* on *myo*-inositol or glucose was not influenced, the growth of WTΔ*iolT1*Δ*iolT2* on *myo*-inositol was disabled but its growth on glucose was not. Consequently, both the *iolT1*- and *iolT2*-encoded carriers appear to catalyze inositol uptake, whereas *mfs1*, although located within the putative *iolA-oxiA* operon (Fig. 3), does not.

Kinetic characterization of IolT1 and IolT2. Cells were grown on CGXII with *myo*-inositol up to an OD_{600} of about 4 to 6, washed twice with CGXII without a carbon source, and stored on ice to quantify *myo*-[1,2-^{3}H]inositol uptake in a rapid filtration assay. Saturation curves were obtained from the initial linear uptake rate (at least three data points over 40 s) at each substrate concentration. For the WT, nonlinear regres-

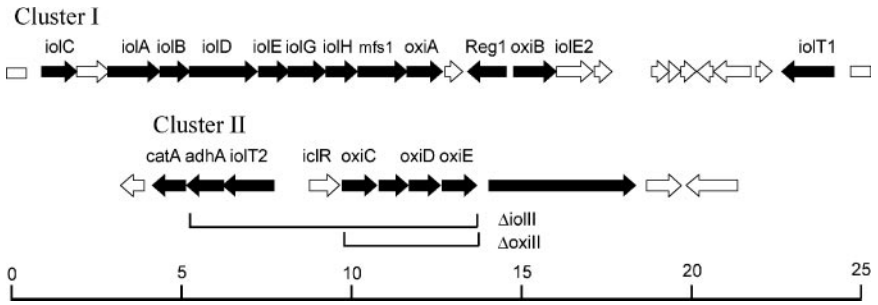

FIG. 3. Genome maps of the *C. glutamicum* regions functioning in *myo*-inositol catabolism. Cluster I shows the genome organization of the nucleotide sequence from 167,768 to 193,453, and cluster II shows the sequence from 3,257,372 to 3,272,564 of the *C. glutamicum* genome NC_003450. Genes exhibiting a ≥2.8-fold increase in the mRNA ratio during growth on *myo*-inositol compared to glucose are in black. Below cluster II, the two genomic deletions Δ*oxiII* and Δ*iolII*, respectively, are indicated. The values on the scale bar are in kilobases.

sion analysis yielded an apparent Michaelis constant (K_m) of 0.20 ± 0.04 mM *myo*-inositol concentration and a V_{max} value of 3.79 ± 0.19 nmol min^{-1} (mg cells)$^{-1}$ (Fig. 4). The mutants with individually deleted IolT1 or IolT2 were analyzed in an identical manner. Assuming that in WTΔ*iolT2* only IolT1 is active, as is indicated by the inability of the double mutant to utilize *myo*-inositol, IolT1 is characterized by a K_m of 0.22 ± 0.04 mM *myo*-inositol and a V_{max} value of 1.22 ± 0.05 nmol min^{-1} (mg cells)$^{-1}$ and IolT2 is characterized by a K_m of 0.45 ± 0.09 mM *myo*-inositol and a V_{max} value of 2.90 ± 0.18 nmol min^{-1} (mg cells)$^{-1}$. Thus, both carriers have comparable kinetic constants, which is probably not surprising since both share a high degree of identity of 55%, although two insertions of up to 15 aminoacyl residues are present in IolT1.

Effect of *myo*-inositol utilization on L-lysine accumulation. *C. glutamicum* is used to satisfy the worldwide demand for L-lysine of more than 600,000 tons per year (8), and it is well known that with the use of fructose or sucrose, L-lysine accumulation is reduced compared to that achieved with glucose (13, 18). Although *myo*-inositol catabolism is only partially known (2, 19, 31), it does not involve complete glycolysis (Fig. 1) and therefore represents an entirely different flux and energetic situation compared to glucose or fructose, for instance.

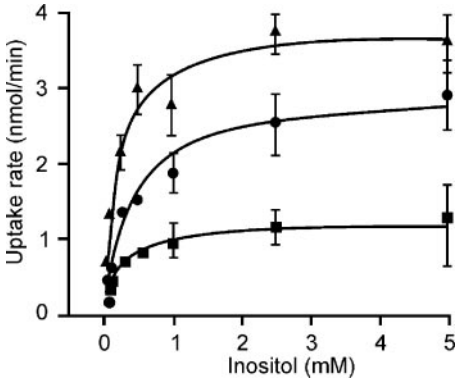

FIG. 4. Substrate saturation kinetics of *myo*-inositol uptake with *C. glutamicum*. Uptake of *myo*-[1,2-^{3}H]inositol by *C. glutamicum* cells was monitored between *myo*-inositol concentrations of 0.05 and 5 mM for 55 s in CGXII by the rapid-filtration technique. From the initial uptake rate at each substrate concentration, the Michaelis-Menten plots were derived by nonlinear regression analysis. Uptake by the WT (▲), the Δ*iolT1* mutant (■), and the Δ*iolT2* mutant (●) is shown.

We grew L-lysine-producing strain *C. glutamicum* DM1730 (13) on salt medium CGXII with glucose and *myo*-inositol as a carbon source, as well as on mixtures of these compounds. After 48 h, the substrates were consumed and the L-lysine concentration was 22.7 mM with *myo*-inositol (Table 3). However, with glucose it was 63.6 mM, which might indicate a reduced supply of the L-lysine building blocks oxaloacetate and pyruvate for L-lysine synthesis. Also with the classically derived L-lysine producer MH20-22B (24), the yields were drastically reduced on *myo*-inositol compared to those achieved with glucose (not shown). Interestingly, even the smallest concentration of 16.6 mM *myo*-inositol added to 186.8 mM glucose reduced the L-lysine yield by 29% (yield of 0.22 instead 0.31), although *myo*-inositol contributed only 8.2% of the total carbon, illustrating a possible regulatory influence of the polyol.

DISCUSSION

It was surprising to find that *myo*-inositol enables such excellent growth of *C. glutamicum*, since similar growth has hardly been reported elsewhere, with the exception of *K.* (*Aerobacter*) *aerogenes* (19). Indeed, the mRNA populations quantified indicate well-balanced growth conditions similar to that on glucose, since only a very limited number of genes are differentially expressed and genes of ribosomal proteins, which

TABLE 3. L-Lysine formation with *C. glutamicum* strain DM1730 as a function of the substrates glucose and *myo*-inositol and mixtures of these substrates

Time[a]	Glucose concn (mM)	Inositol concn (mM)	Growth (OD)	L-Lysine[b] concn (mM)	Yield[c] (mol/mol)
I	202.0	0	14	37.8	0.19
I	186.8	16.6	24	40.5	0.20
I	176.7	27.7	23	38.1	0.19
I	0	222.0	17	23.0	0.10
II	202.0	0	21	63.6	0.31
II	186.8	16.6	23	44.1	0.22
II	176.7	27.7	24	38.3	0.19
II	0	222.0	19	22.7	0.10

[a] Time I gives growth, L-lysine concentration, and yield after 24 h, whereas time II gives the values after 48 h, when all of the sugar was consumed.

[b] All data are mean values of at least three independent cultivations with errors of <5% for L-lysine concentrations and yields.

[c] Molar yields are given as moles of L-lysine per mole of carbon source consumed.

often respond to starvation conditions, are absent (14). The most strongly downregulated gene is *ips*, and it is logical to assume that this is a direct consequence of the presence of *myo*-inositol. Although the mechanism of regulation is still to be discovered, regulation of *ips* opens up the possibility of controlling lipomannan and lipoarabinomannan synthesis as an interesting target for reducing the viability of *Corynebacterineae* such as *M. tuberculosis* (5) by the synthesis of these *myo*-inositol-containing glycolipids.

The number of genes exhibiting increased expression upon *myo*-inositol catabolism was puzzling at the beginning of our work, in particular since knowledge of *myo*-inositol utilization in general is rather limited. Thus, according to the array analysis, in principle, as many as six oxidoreductases could be required for *myo*-inositol utilization, as well as three transporters and two isomerase-epimerases (Table 2). However, the deletion of all of cluster II and growth of the corresponding mutant WTΔ*iolII* are strong evidence that cluster II encodes redundant functions of *myo*-inositol utilization as specifically demonstrated for uptake and oxidation steps within the catabolism of the polyol. Moreover, the genomic region of cluster II encompassing the adjacent *catA-adh* region exhibits amazingly high identities at the nucleotide level of up to 74% to NCgl1112 and NCgl1113, located elsewhere in the chromosome, showing that gene duplication within *C. glutamicum* might also be involved in the formation of cluster II. Also the high identity of 30% between *oxiD* and *oxiE* at the protein level and even at the nucleotide level (not shown) illustrates that this genomic region does not belong to regions encoding conserved cellular core functions like cell wall synthesis, for instance (1, 12). Instead, this region appears to be rather the result of a more recent event of genome alteration. This is in full accord with the absence of *iol* genes in *C. efficiens*, *C. diphtheriae*, and *C. jeikeium* indicating a specific and fortuitous acquisition of these genes by *C. glutamicum*.

Cluster I encodes relevant functions for *myo*-inositol catabolism in *C. glutamicum*, as evident from the consequences of *iolD* inactivation and the *iolG* mutation in the Δ*oxi*II background. As evident from the early biochemical work of Magasanik and coworkers (2, 19), *myo*-inositol catabolism might involve oxidative steps, epimerization, phosphorylation of a linear diketo-deoxy-inositol, cleavage, and a further oxidative step to yield acetyl-CoA and dihydroxyacetone-P (Fig. 1). Interestingly, orthologues of six genes of cluster I are present and largely syntenic to the organization of *C. glutamicum* in *B. subtilis* (29), *B. halodurans*, *Clostridium perfringens* (17), and *Yersinia pseudotuberculosis*. Therefore, these genes are likely to encode the key functions to catabolize *myo*-inositol, as discussed in detail by Magasanik. This relates to *iolG* and *iolE*, whose functions have been identified (10, 31); to *iolC*, whose structural characteristics according to PFAM analysis (3) indicate that it encodes a 5-dehydro-2-deoxygluconokinase; *iolD*, which encodes a thiamine pyrophosphate-dependent enzyme typically cleaving sugar phosphates; and *iolA*, which encodes an aldehyde dehydrogenase. The *iolB*-encoded protein is also conserved but does not have a PFAM entry, consequently representing a protein with no structural counterpart in the current databases. The initial oxidative steps to form a cleavable diketo intermediate from *myo*-inositol might differ among the bacteria. At least the genome comparisons did not allow us to specify a core requirement for oxidoreductases.

Uptake of *myo*-inositol to sustain maximal growth is possible by either IolT1 or IolT2, and the genes for both are expressed to similar degrees (Table 2). They also have comparable kinetic properties, which is probably not surprising due to their high sequence identity of 55%. The IolT proteins are 12-membrane spanners belonging to the major facilitator superfamily. Also, *B. subtilis* has two inositol uptake carriers that are similar in structure, but these share fewer sequence identities than do the *C. glutamicum* proteins. In marked contrast to *C. glutamicum*, in *B. subtilis* neither transporter can be substituted for the other since they represent a minor and a major *myo*-inositol transporter (28). It is surprising that the third transporter of *C. glutamicum* analyzed in the present study is part of cluster I but nevertheless is not involved in *myo*-inositol uptake. Instead, it shares identities with efflux pumps, indicating together with its absence in the *iol* locus of other bacteria, its fortuitous presence in cluster I.

The L-lysine formation data showed a reduced yield with *myo*-inositol as a carbon source compared to glucose. It is known that the amino acid yield strongly depends on the type of substrate. The highest L-lysine yields with *C. glutamicum* are obtained with glucose, and the lowest are obtained with fructose (13, 18). Thus, *myo*-inositol ranks among the substrates giving rather low yields. This could be due to the fact that pyruvate and oxaloacetate, required as building blocks for L-lysine, probably do not result from *myo*-inositol catabolism (2, 19). Surprising is the fact that there is a significant yield reduction when *myo*-inositol is present at relatively low supplementary concentrations in addition to glucose. Although *myo*-inositol contributes about 8% of the total carbon in a mixture with glucose, the resulting yield is reduced by as much as 29% (Table 3). The effect of cells grown in different complex media and used as inoculum on the final yield is well established (25), and the present study, as well as a proteome study (15), shows that *iol* genes are expressed on complex media usually used to derive the inoculum. However, in our experiments the preculture medium for deriving the inoculum was identical to the culture medium where the yields were determined. We envisage two possibilities. Although we did no DNA microarray analysis for cells grown on a glucose-inositol mixture, *myo*-inositol undoubtedly affects expression of genes of central metabolism, like components of the phosphotransferase system (see above), as well as *mez*, malic enzyme, or *sucC*, encoding a succinyl-CoA synthetase subunit (Table 2). Moreover, enzyme activities could be influenced by different metabolite concentrations. The other possibility is that due to the presence of *myo*-inositol the cell wall and its lipomannan composition are influenced so as to reduce L-lysine export. It is known that in *C. glutamicum* the cellular lipid composition influences amino acid efflux properties (6).

REFERENCES

1. **Alderwick, L. J., M. Seidel, H. Sahm, G. S. Besra, and L. Eggeling.** 2006. Identification of a novel arabinofuranosyl transferase (AftA) involved in cell wall arabinan biosynthesis in *Mycobacterium tuberculosis*. J. Biol. Chem. **281:**15653–15661.
2. **Anderson, W. A., and B. Magasanik.** 1971. The pathway of *myo*-inositol degradation in *Aerobacter aerogenes*. J. Biol. Chem. **246:**5662–5675.
3. **Bateman, A., L. Coin, R. Durbin, R. D. Finn, V. Hollich, S. Griffiths-Jones, A. Khanna, M. Marshall, S. Moxon, E. L. Sonnhammer, D. J. Studholme, C.**

Yeats, and S. R. Eddy. 2004. The Pfam protein families database. Nucleic Acids Res. **32:**D138–D141.
4. **Bellmann, A., M. Vrljic, M. Patek, H. Sahm, R. Krämer, and L. Eggeling.** 2001. Expression control and specificity of the basic amino acid exporter LysE of *Corynebacterium glutamicum*. Microbiology **147:**1765–1774.
5. **Brennan, P. J., and H. Nikaido.** 1995. The envelope of mycobacteria. Annu. Rev. Biochem. **64:**29–63.
6. **Eggeling, L., and H. Sahm.** 2001. The cell wall barrier of *Corynebacterium glutamicum* and amino acid efflux. J. Biosci. Bioeng. **92:**201–213.
7. **Eggeling, L., and H. Sahm.** 1985. The formaldehyde dehydrogenase of *Rhodococcus erythropolis*, a trimeric enzyme requiring a cofactor and active with alcohols. Eur. J. Biochem. **150:**129–134.
8. **Eggeling, L., and M. Bott.** 2005. Handbook of *Corynebacterium glutamicum*. CRC Press, Inc., Boca Raton, Fla.
9. **Fry, J., M. Wood, and P. S. Poole.** 2001. Investigation of *myo*-inositol catabolism in *Rhizobium leguminosarum* bv. *viciae* and its effect on nodulation competitiveness. Mol. Plant-Microbe Interact. **14:**1016–1025.
10. **Fujita, Y., K. Shindo, Y. Miwa, and K. Yoshida.** 1991. *Bacillus subtilis* inositol dehydrogenase-encoding gene (*idh*): sequence and expression in *Escherichia coli*. Gene **108:**121–125.
11. **Galbraith, M. P., S. F. Feng, J. Borneman, E. W. Triplett, F. J. de Bruijn, and S. Rossbach.** 1998. A functional *myo*-inositol catabolism pathway is essential for rhizopine utilization by *Sinorhizobium meliloti*. Microbiology **144:**2915–2924.
12. **Gande, R., K. J. Gibson, A. K. Brown, K. Krumbach, L. G. Dover, H. Sahm, S. Shioyama, T. Oikawa, G. S. Besra, and L. Eggeling.** 2004. Acyl-CoA carboxylases (*accD2* and *accD3*), together with a unique polyketide synthase (Cg-*pks*), are key to mycolic acid biosynthesis in *Corynebacterineae* such as *Corynebacterium glutamicum* and *Mycobacterium tuberculosis*. J. Biol. Chem. **279:**44847–44857.
13. **Georgi, T., D. Rittmann, and V. F. Wendisch.** 2005. Lysine and glutamate production by *Corynebacterium glutamicum* on glucose, fructose and sucrose: roles of malic enzyme and fructose-1,6-bisphosphatase. Metab. Eng. **7:**291–301.
14. **Gourse, R. L., T. Gaal, M. S. Bartlett, J. A. Appleman, and W. Ross.** 1996. rRNA transcription and growth rate-dependent regulation of ribosome synthesis in *Escherichia coli*. Annu. Rev. Microbiol. **50:**645–677.
15. **Hansmeier, N., T. C. Chao, A. Pühler, A. Tauch, and J. Kalinowski.** 2006. The cytosolic, cell surface and extracellular proteomes of the biotechnologically important soil bacterium *Corynebacterium efficiens* YS-314 in comparison to those of *Corynebacterium glutamicum* ATCC 13032. Proteomics **6:**233–250.
16. **Jiang, G., A. H. Krishnan, Y.-W. Kim, T. J. Wacek, and H. B. Krishnan.** 2001. A functional *myo*-inositol dehydrogenase gene is required for efficient nitrogen fixation and competitiveness of *Sinorhizobium fredii* USDA191 to nodulate soybean (*Glycine max* [L.] Merr.). J. Bacteriol. **183:**2595–2604.
17. **Kawsar, H. I., K. Ohtani, K. Okumura, H. Hayashi, and T. Shimizu.** 2004. Organization and transcriptional regulation of myo-inositol operon in *Clostridium perfringens*. FEMS Microbiol. Lett. **235:**289–295.
18. **Kiefer, P., E. Heinzle, O. Zelder, and C. Wittmann.** 2004. Comparative metabolic flux analysis of lysine-producing *Corynebacterium glutamicum* cultured on glucose or fructose. Appl. Environ Microbiol. **70:**229–239.
19. **Magasanik, B.** 1953. Enzymatic adaptation in the metabolism of cyclitols in *Aerobacter aerogenes*. J. Biol. Chem. **205:**1007–1018.
20. **Norman, R. A., M. S. McAlister, J. Murray-Rust, F. Movahedzadeh, N. G. Stoker, and N. Q. McDonald.** 2002. Crystal structure of inositol 1-phosphate synthase from *Mycobacterium tuberculosis*, a key enzyme in phosphatidylinositol synthesis. Structure **10:**393–402.
21. **Sambrook, J., E. F. Fritsch, and T. Maniatis.** 1989. Molecular cloning: a laboratory manual, 2nd ed. Cold Spring Harbor Laboratory Press, Cold Spring Harbor, N.Y.
22. **Sareen, D., G. L. Newton, R. C. Fahey, and N. A. Buchmeier.** 2003. Mycothiol is essential for growth of *Mycobacterium tuberculosis* Erdman. J. Bacteriol. **185:**6736–6740.
23. **Schäfer, A., A. Tauch, W. Jäger, J. Kalinowski, G. Thierbach, and A. Pühler.** 1994. Small mobilizable multi-purpose cloning vectors derived from the *Escherichia coli* plasmids pK18 and pK19: selection of defined deletions in the chromosome of *Corynebacterium glutamicum*. Gene **145:**69–73.
24. **Schrumpf, B., L. Eggeling, and H. Sahm.** 1992. Isolation and prominent characteristics of an L-lysine hyperproducing strain of *Corynebacterium glutamicum*. Appl. Microbiol. Biotechnol. **37:**566–571.
25. **Sonntag, K., L. Eggeling, A. A. De Graaf, and H. Sahm.** 1993. Flux partitioning in the split pathway of lysine synthesis in *Corynebacterium glutamicum*. Quantification by ^{13}C- and ^{1}H-NMR spectroscopy. Eur. J. Biochem. **213:**1325–1331.
26. **Turner, B. L., and A. L. Richardson.** 2004. Identification of *scyllo*-inositol phosphates in soil by solution phosphorus-31 nuclear magnetic resonance spectroscopy. Soil Sci. Soc. Am. J. **68:**802–808.
27. **Wendisch, V. F.** 2003. Genome-wide expression analysis in *Corynebacterium glutamicum* using DNA microarrays. J. Biotechnol. **104:**273–285.
28. **Yoshida, K., Y. Yamamoto, K. Omae, M. Yamamoto, and Y. Fujita.** 2002. Identification of two myo-inositol transporter genes of *Bacillus subtilis*. J. Bacteriol. **184:**983–991.
29. **Yoshida, K.-I., D. Aoyama, I. Ishio, T. Shibayama, and Y. Fujita.** 1997. Organization and transcription of the *myo*-inositol operon, *iol*, of *Bacillus subtilis*. J. Bacteriol. **179:**4591–4598.
30. **Yoshida, K., K. Kobayashi, Y. Miwa, C.-M. Kang, M. Matsunaga, H. Yamaguchi, S. Tojo, M. Yamamoto, R. Nishi, N. Ogasawara, T. Nakayama, and Y. Fujita.** 2001. Combined transcriptome and proteome analysis as a powerful approach to study genes under glucose repression in *Bacillus subtilis*. Nucleic Acids Res. **29:**683–692.
31. **Yoshida, K., M. Yamaguchi, H. Ikeda, K. Omae, K. Tsurusaki, and Y. Fujita.** 2004. The fifth gene of the *iol* operon of *Bacillus subtilis*, *iolE*, encodes 2-keto-myo-inositol dehydratase. Microbiology **150:**571–580.